



Received on 06 September 2019; received in revised form, 12 August 2020; accepted, 14 August 2020; published 01 September 2020

## QSAR STUDIES, SYNTHESIS AND BIOLOGICAL EVALUATION OF PYRAZOLE DERIVATIVES CONTAINING THIOUREA AS TYROSINE KINASE INHIBITORS: AN APPROACH TO DESIGN ANTICANCER AGENTS

Asheesh Singh\* and P. K. Singour

Computational & Synthetic Chemistry Division, Department of Pharmaceutical Chemistry, VNS Faculty of Pharmacy, Bhopal - 462026, Madhya Pradesh, India.

### Keywords:

QSAR, Tyrosine Kinase,  
Pyrazole, Anti-cancer, EGFR

### Correspondence to Author:

**Asheesh Singh**

Research Scholar,  
Computational & Synthetic  
Chemistry Division, Department of  
Pharmaceutical Chemistry, VNS  
Faculty of Pharmacy, Bhopal -  
462026, Madhya Pradesh, India.

**E-mail:** asheesh\_parihar@yahoo.com

**ABSTRACT:** A series of pyrazole derivatives designing for potential EGFR kinase inhibitors have been discovered. Some of them exhibited significant EGFR inhibitory activity. Compound 3-(4-Amino-phenyl)-5-(3-nitro-phenyl)-4, 5-dihydro-pyrazole-1-carbothioic acid amide (AP-2) displayed the most potent EGFR inhibitory activity. The QSAR analysis of a set of these compounds tested for growth inhibitory activity against EGFR were performed by using the computer-assisted multiple regression procedure. The activity contributions for substituent effects of these compounds were determined from the correlation equation for predictions of the lead optimization. QSAR analysis of these compounds was performed by multiple regression analysis in order to predict the lead optimization for anticancer activity against EGFR.

**INTRODUCTION:** Cancer, the uncontrolled, rapid and pathological proliferation of abnormal cells, is the second leading cause of human death after cardiovascular diseases in developing as well as advanced countries<sup>1</sup>. Cancer may affect people at all ages, even fetuses, but the risk for the more common varieties tends to increase with age. Cancer causes about 13% of all deaths. Nearly all cancers are caused by abnormalities in the genetic material of the transformed cells. These abnormalities may be due to the effects of carcinogens, such as tobacco smoke, radiation, chemicals, or infectious agents.

Other cancer-promoting genetic abnormalities may be randomly acquired through errors in DNA (Deoxyribonucleic acid) replication or are inherited and thus present in all cells from birth. However, there are many therapeutic strategies, including chemotherapy and radiotherapy, high systemic toxicity, and drug resistance, to limit the successful outcomes in most cases.

Therefore, novel diagnosis, treatment, and prevention approaches are urgently needed for cancer therapy<sup>2-3</sup>. Cancer chemotherapy has entered a new era of molecularly targeted therapeutics, which is highly selective and not associated with the serious toxicities of conventional cytotoxic drugs. Receptor protein tyrosine kinases play a key role in signal transduction pathways that regulate cell division and differentiation. Among the growth factor receptor kinases that have been identified as being important in cancer is epidermal growth factor

<p><b>QUICK RESPONSE CODE</b></p> 	<p><b>DOI:</b> 10.13040/IJPSR.0975-8232.11(9).4388-94</p> <hr/> <p>This article can be accessed online on <a href="http://www.ijpsr.com">www.ijpsr.com</a></p> <hr/> <p>DOI link: <a href="http://dx.doi.org/10.13040/IJPSR.0975-8232.11(9).4388-94">http://dx.doi.org/10.13040/IJPSR.0975-8232.11(9).4388-94</a></p>
---	---

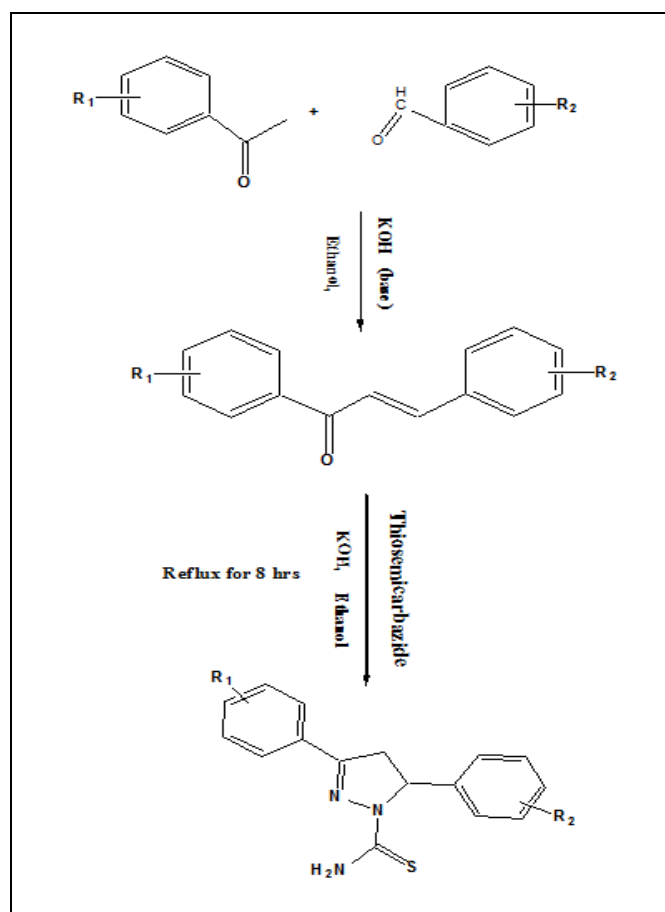
receptor (EGFR) kinase. Activation of EGFR may be because of overexpression, mutations resulting in constitutive activation, or autocrine expression of the ligand. The role of EGFR has been most thoroughly studied in breast cancer, where it is overexpressed in 25–30% of cases and is correlated with a poor prognosis. EGFR overexpression is also seen in ovarian cancer<sup>4</sup>. The thiourea and urea derivatives play an important role in anticancer agents because of their good inhibitory activity against receptor tyrosine kinases (RTKs), protein tyrosine kinases (PTKs) and NADH oxidase, which play critical roles in many aspects of tumorigenesis. Many pyrazole derivatives are acknowledged to possess a wide range of bioactivities.

The pyrazole motif makes up the core structure of numerous biologically active compounds. Thus, some representatives of this heterocycle exhibit anti-viral/anti-tumor. Much attention was paid to pyrazole as a potential antimicrobial agent after the discovery of the natural pyrazole C-glycoside, pyrazofurin which demonstrated a broad spectrum of antimicrobial activity. However, to our knowledge, few reports have been dedicated to the synthesis and EGFR inhibitory activity of pyrazole derivatives containing thiourea skeleton<sup>5-6</sup>.

The investigation of the quantitative structure-activity relationships (QSAR) of substances is an important aspect of modern chemistry, biochemistry, medicinal chemistry, and drug discovery. The information obtained is composed of mathematical equations relating the chemical structure of the compounds to a wide variety of their physical, chemical, biological, and technological properties. Once a correlation between structure and activity/property is found, any number of compounds, including those not synthesized yet, can readily be screened for selection of structures with desired properties. Hence, it is possible to select the most promising compounds for synthesis and testing in laboratory<sup>7-11</sup>.

In this research, some novel Pyrazole derivatives were synthesized in order to interpret their anticancer activity against EGFR. The 2D-QSAR analysis was also aimed to explain clearly the relation of physicochemical parameters with the activity.

**CHEMISTRY:** The synthesis of compounds AP1–AP10 followed the general pathway outlined in **Scheme 1**. They are prepared in two steps. Firstly, the chalcones were obtained by direct condensation between the aromatic aldehydes and the substituted acetophenone, using 20% potassium hydroxide as a catalyst in ethanol. Secondly, for compounds AP1–AP10, cyclization of different chalcones with thiosemicarbazide under the basic condition in refluxing ethanol leads to the formation of pyrazole derivatives containing thiourea skeleton. All of the synthetic compounds gave satisfactory analytical and spectroscopic data, which were in full accordance with their depicted structures.



**SCHEME 1: REAGENT AND CONDITIONS: (I) SUBSTITUTED AROMATIC ALDEHYDES, 40% NaOH, CH<sub>3</sub>CH<sub>2</sub>OH; (II) THIOSEMICARBAZIDE, CH<sub>3</sub>CH<sub>2</sub>OH, REFLUX**

**RESULTS AND DISCUSSION:** Four statistically significant QSAR models have been developed by using multiple linear regression analysis.

**Model 1:** BA = [29.8216 (± 3.81837)] +Homo [2.76231 (± 0.431208)] +Nonvdw [3.69903 (± 1.42212)] + P<sub>mix</sub> [-8.30969 (± 3.39441)]

$N = 32$ ,  $r = 0.7815$ ,  $r^2 = 0.6107$ ,  $r^2_{adj} = 0.5690$ , variance = 0.1530, std = 0.3911, QF = 1.9980, PE = 0.04589, F = 14.6409, FIT = 1.0713, LOF = 7.0177, AIC = 0.1967

Model 1 explains only 61.2% variance in the anticancer activity. It shows that descriptor Highest occupied molecular orbital (HOMO) and Non Vander walls (NonVDW) contribute positively, where as principal moment of inertia x (Pmix) contribute negatively towards anticancer activity. It is not a very good significant equation, therefore new model required for good explained variance.

**Model 2:**  $BA = [3.21588 (\pm 1.27474)] + Mw [-0.010452 (\pm 0.00158041)] + Cnsev [-0.0442412 (\pm 0.00871579)] + MR [0.18273 (\pm 0.0241215)]$

$N = 31$ ,  $r = 0.830432$ ,  $r^2 = 0.6896$ ,  $r^2_{adj} = 0.65513$ , variance = 0.0791235, std = 0.281289, QF = 2.95224, PE = 0.0371643, F = 19.9964, FIT = 1.51734, LOF = 3.56427, AIC = 0.098097

Model 2 explains only 68.9% variance in the anticancer activity. It shows that descriptor molecular weight (MW) and Connolly solvent excluded volume (Cnsev) contribute negatively; whereas Molar refractivity (MR) contributes positively towards anticancer activity. In this model one compound (5) was outlier. It is not a very good significant equation, therefore new model required for good explained variance.

**Model 3:**  $BA = [3.17486 (\pm 0.873342)] + Ectms [-0.0080589 (\pm 0.00119124)] + Cnsev [-0.034357 (\pm 0.00621457)] + MR [0.145844 (\pm 0.0177856)]$   $N = 30$ ,  $r = 0.85377$ ,  $r^2 = 0.728924$ ,  $r^2_{adj} = 0.697646$ , variance = 0.0371608, std = 0.192771, QF = 4.42893, PE = 0.0329943, F = 23.3047, FIT = 1.83639, LOF = 1.64378, AIC = 0.0443654

Model 3 explains only 72.8% variance in the anticancer activity. It shows that descriptor Exact mass (Ectms) and Connolly solvent excluded volume (Cnsev) contribute negatively, whereas molecular refractivity (MR) contributes positively towards the anticancer activity.

In this model, two compounds (1 and 4) were outliers. It is not a very good significant equation, therefore a new model required for a well-explained variance.

**Model 4:**  $BA = [3.87157(\pm 0.429843)] + MW [-0.0040636(\pm 0.000697125)] + Cnsev [-0.0243882 (\pm 0.00313334)] + MR [0.0947197 (\pm 0.010074)]$   $N = 27$ ,  $r = 0.9115$ ,  $r^2 = 0.8309$ ,  $r^2_{adj} = 0.8087$ , variance = 0.0081, std = 0.0901, QF = 10.1107, PE = 0.0217, F = 37.6459, FIT = 3.3534, LOF = 0.3407, AIC = 0.0086

Model 4 explains 83.1% variance in the anticancer activity with a low standard error shows the relative good fitness of the model. It shows that molecular descriptor weight (MW) and Connolly solvent excluded volume (Cnsev) contribute negatively, whereas molar refractivity (MR) contributes positively towards the anticancer activity. In this model, two compounds 1, 2, 3, 4, and 5 were outliers. Molar refractivity (MR), a steric parameter, which is positively correlated, indicates that sterically bulky substituent would increase the binding affinity. The graph between experimental and predicted biological activity of training set compounds by using model 4 is shown in **Fig. 1**. The validation criteria for the selection of the model are cross-validated squared correlation coefficient ( $q^2$ ). The cross-validation correlation coefficient ( $q^2$ ) was 0.7644 means model 4 has good predictive power. The graph between experimental BA and predicted BA of test set compounds by using model 4 is shown in **Fig. 2**. Show mutual correlation among the parameters.

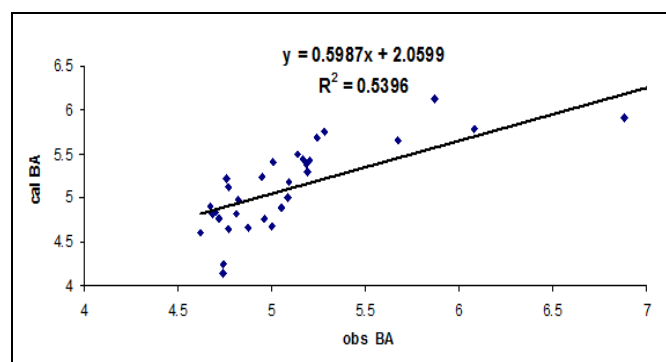


**FIG. 1: EXPERIMENTAL vs. PREDICTED BIOLOGICAL ACTIVITY (BA) OF TRAINING SET COMPOUNDS BY MULTIPLE LINEAR REGRESSION MODEL**

A series of pyrazole derivatives have been synthesized by using a two-step procedure, as shown in Scheme 1. All of the derivatives were supported by spectral data. The IR,  $^1H$  NMR and mass spectra are in agreement with the proposed structures. Physical and spectral data of the compounds are reported in experimental Section.

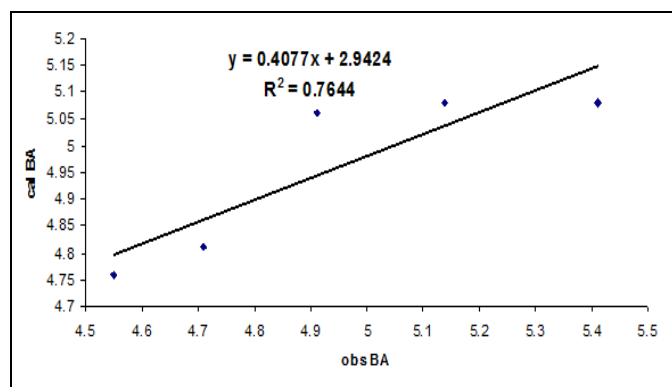


FIG. 2: EXPERIMENTAL vs. PREDICTED BIOLOGICAL ACTIVITY (BA) OF TEST SET COMPOUNDS BY MULTIPLE LINEAR REGRESSION MODEL

**Experimental:** The data set of 37 molecules with their anticancer activity has been taken from the published results<sup>4</sup>. Anticancer activity was expressed as  $IC_{50}$  ( $\mu\text{m}$ ) values, which were converted into  $-\log IC_{50}$  for the convenience of computational work. It is essential to assess the predictive power of the models by using a test set of compounds. This was achieved by arbitrarily setting aside some compounds as a test set.

**Molecular Structure Generation:** All structure of pyrazole derivatives compounds were constructed using Chemoffice 2003 version 6.0 software supplied by Cambridge Software Company, USA. All 2D (2-Dimensional) structure is converted into 3D (3-Dimensional) structures in Chem 3D in Chemoffice 2003 (CS Chem Office version 6.0).

**Energy Minimization:** The resulting 3D structures were then subjected to an energy-minimization process by using the molecular mechanics (MM2) method was applied to search for lower energy conformations for each molecule. The energy minimized molecules were re-optimizing using a molecular orbital package (MOPAC).

**Descriptors Calculation:** The energy minimizes structures were used for calculating various physicochemical descriptors like thermodynamic, electronic, steric, and topological. Thermodynamic parameters describe free energy change during drug-receptor complex formation.

Spatial parameters are the quantified steric features of drug molecules required for their complementary fit with the receptor. Electronic parameters describe weak non-covalent bonding between drug molecules and receptors.

**Statistical Analysis:** All the data sets (37 molecules) were divided into two sets. The first one training set having 32 molecules for the generation of QSAR models, and a second test set is having 5 molecules for validation of generated QSAR models. VALSTAT software was used to generate QSAR models by multiple linear regression analysis. Cross-validation was performed using the leave-one-out method. For multiple linear regression analysis, biological activity ( $-\log IC_{50}$ ) values were used as dependent variables and calculated parameters (descriptors) used as independent variables. The inter-correlation between the parameters was less than 0.5, which shows inter-pair correlations among the selected descriptors are very low. Acceptability of the regression model was judged by examining the different statistical parameters *i.e.*, number of samples in regression ( $n$ ), regression coefficient ( $r$ ), squared regression coefficient ( $r^2$ ), adjusted squared regression coefficient ( $r^2$  adj), F-test (Fischer's value) for statistical significance, standard deviation (std), cross-validated squared correlation coefficient ( $q^2$ ), bootstrapped squared correlation coefficient ( $bsr^2$ ), Friedman lack of fit measure (LOF), quality factor (QF), probable Error of correlation (PE), Kubinyi function (FIT), Akaike's Information Criterion (AIC) and correlation matrix to show a mutual correlation among the parameters.

**Chemistry:** Common reagent grade chemicals for the synthesis were purchased either from Sigma Chemical Co., St. Louis, Missouri, USA or Merck Chemicals, India, and were used as received. The purity of the synthesized compounds was confirmed by thin-layer chromatography (TLC) using silica gel-G, solvent system chloroform: ethyl acetate: formic acid (5:4:1) as mobile phase and iodine vapor as detecting agent. The melting points of synthesized compounds were determined by the VEEGO melting point apparatus and are uncorrected. IR spectra were recorded on FTIR, 2000A, ABB spectrophotometer ( $ZrCl_2$ ).  $^1H$  NMR spectra of the synthesized compounds were recorded on Bruker WM 200 MHz Spectrometer in  $CDCl_3$  solvent with TMS as internal standard. The electron spray mass spectra were recorded on a triple quadrupole mass spectrometer. EI mass spectra were recorded on the JEOL JMS-D-300 spectrometer with the ionization potential of 70 eV.

**General Procedure for Synthesis of Compounds:**  
**General Synthetic Procedure of Chalcone:** Equimolar portions of the appropriately substituted aromatic aldehydes (4 mol, 1 equiv) and ketones (4 mol, 1 equiv) were dissolved in approximately 15 mL of ethanol. The mixture was allowed to stir for several minutes at 5–10 °C. A 10 mL aliquot of a 40% aqueous potassium hydroxide solution was then slowly added dropwise to the reaction flask via a self-equalizing addition funnel. The reaction solution was allowed to stir at room temperature for approximately 4 h. Most commonly, a precipitate formed and was then collected by suction filtration.

**General Synthetic Procedure of Pyrazole Derivatives AP1-AP10:** A mixture of chalcone (1 mol), thiosemicarbazide (0.01 mol), and KOH (0.025 mol) was refluxed in ethanol (25 mL) for 8 h. The solution was poured into ice-water. The precipitate was filtered and crystallized from methanol.

**3-(4-Amino-phenyl)-5-(4-chloro-phenyl)-4,5-dihydro-pyrazole-1-carbothioic Acid Amide (AP-1):**  $C_{16}H_{15}ClN_4S$  - M.P.: 282-284 °C; Yield (%): 24; UV ( $\lambda_{max}$ ): 344.5;  $^1H$  NMR (ppm): 2.0 (s, 2H, S=C-NH<sub>2</sub>), 4.0 (t, 2H, H<sub>4</sub>C<sub>6</sub>-NH<sub>2</sub>), 1.9 (d, 2H, -CH<sub>2</sub>- 4,5-dihydropyrazole), 3.9 (m, 1H, -CH- 4,5-dihydropyrazole), 6.5-7.4 (m, 4H, =CH-benzylidinimin), 7.06-7.22 (m, 4H, =CH-benzene); IR ( $cm^{-1}$ ) 3329 (N-H), 2975 (C-H), 1652 & 1457 (C=C Ar), 1419 (C-N), 1216 (C=S), 785 (C-Cl); MS (70 eV) m/z: (M+), 330.07 (100%).

**3-(4-Amino-phenyl)-5-(3-nitro-phenyl)-4,5-dihydro-pyrazole-1-carbothioic Acid Amide (AP-2):**  $C_{16}H_{15}N_5O_2S$  - M.P.: 320-322 °C; Yield (%): 36; UV ( $\lambda_{max}$ ): 342.5;  $^1H$  NMR (ppm): 2.0 (s, 2H, S=C-NH<sub>2</sub>), 4.0 (t, 2H, H<sub>4</sub>C<sub>6</sub>-NH<sub>2</sub>), 1.9 (d, 2H, -CH<sub>2</sub>- 4,5-dihydropyrazole), 3.9 (m, 1H, -CH- 4,5-dihydropyrazole), 6.5-7.4 (m, 4H, =CH-benzylidinimin), 7.51-8.05 (m, 4H, =CH-benzene); IR ( $cm^{-1}$ ) 3420 (N-H), 2970 (C-H), 1606 & 1480 (C=C Ar), 1590 (C=N), 1550 & 1350 (NO<sub>2</sub>), 1337 (C-N), 1216 (C=S); MS (70 eV) m/z: (M+), 341.09 (100%).

**3-(4-Amino-phenyl)-5-(3,4-dimethoxy-phenyl)-4,5-dihydro-pyrazole-1-carbothioic Acid Amide (AP-3):**  $C_{18}H_{20}N_4O_2S$  - M.P.: 340-342 °C; Yield (%): 48; UV ( $\lambda_{max}$ ): 340.5;  $^1H$  NMR (ppm): 2.0 (s,

2H, S=C-NH<sub>2</sub>), 4.0 (t, 2H, H<sub>4</sub>C<sub>6</sub>-NH<sub>2</sub>), 1.9 (d, 2H, -CH<sub>2</sub>- 4,5-dihydropyrazole), 3.9 (m,  $^1H$ , -CH- 4,5-dihydropyrazole), 3.73 (s, 6H, -(O-CH<sub>3</sub>)<sub>2</sub>), 6.5-7.4 (m, 4H, =CH-benzylidinimin), 6.52-6.61 (m, 4H, =CH-benzene); IR ( $cm^{-1}$ ) 3420 (N-H), 2970 (C-H), 1559 & 1436 (C=C Ar), 1365 (C-N), 1228 (C-O), 1216 (C=S); MS (70 eV) m/z: (M+), 356.13 (100%).

**3-(4-Amino-phenyl)-5-(4-dimethylamino-phenyl)-4,5-dihydro-pyrazole-1-carbothioic Acid Amide (AP-4):**  $C_{18}H_{21}N_5S$  - M.P.: 350 °C; Yield (%): 40; UV ( $\lambda_{max}$ ): 370.5;  $^1H$  NMR (ppm): 2.0 (s, 2H, S=C-NH<sub>2</sub>), 4.0 (t, 2H, H<sub>4</sub>C<sub>6</sub>-NH<sub>2</sub>), 1.9 (d, 2H, -CH<sub>2</sub>- 4,5-dihydropyrazole), 2.85 (s, 6H, -N-(CH<sub>3</sub>)<sub>2</sub>), 3.9 (m,  $^1H$ , -CH- 4,5-dihydropyrazole), 6.5-7.4 (m, 4H, =CH-benzylidinimin), 6.54-6.94 (m, 4H, =CH-benzylidinimin); IR ( $cm^{-1}$ ) 3410 (N-H), 2970 (C-H), 1595 & 1417 (C=C Ar), 1541 (C=N), 1216 (C=S); MS (70 eV) m/z: (M+), 339.15 (100%).

**3-(4-Amino-phenyl)-5-(4-dimethoxy-phenyl)-4,5-dihydro-pyrazole-1-carbothioic Acid Amide (AP-5):**  $C_{17}H_{18}N_4OS$  - M.P.: 358-360 °C; Yield (%): 52; UV ( $\lambda_{max}$ ): 333;  $^1H$  NMR (ppm): 2.0 (s, 2H, S=C-NH<sub>2</sub>), 4.0 (t, 2H, H<sub>4</sub>C<sub>6</sub>-NH<sub>2</sub>), 1.9 (d, 2H, -CH<sub>2</sub>- 4,5-dihydropyrazole), 3.9 (m, 1H, -CH- 4,5-dihydropyrazole), 3.73 (s, 6H, -(O-CH<sub>3</sub>)<sub>2</sub>), 6.5-7.4 (m, 4H, =CH-benzylidinimin), 6.72-7.01 (m, 4H, =CH-benzene); IR ( $cm^{-1}$ ) 3364 (N-H), 2925 (C-H), 1597 & 1467 (C=C Ar), 1508 (C=N), 1299 (C-O), 1248 (C=S); MS (70 eV) m/z: (M+), 326.12 (100%).

**3-(4-Amino-phenyl)-5-(4-fluoro-phenyl)-4,5-dihydro-pyrazole-1-carbothioic Acid Amide (AP-6):**  $C_{16}H_{15}N_4FS$  - M.P.: 316 °C; Yield (%): 48; UV ( $\lambda_{max}$ ): 313;  $^1H$  NMR (ppm): 2.0 (s, 2H, S=C-NH<sub>2</sub>), 4.0 (t, 2H, H<sub>4</sub>C<sub>6</sub>-NH<sub>2</sub>), 1.9 (d, 2H, -CH<sub>2</sub>- 4,5-dihydropyrazole), 3.9 (m, 1H, -CH- 4,5-dihydropyrazole), 6.5-7.4 (m, 4H, =CH-benzylidinimin), 6.52-6.61 (m, 4H, =CH-benzene); IR ( $cm^{-1}$ ) 3375 (N-H), 2873 (C-H), 1954 & 1417 (C=C Ar), 1508 (C=N), 1226 (C=S), 999 (C-F), MS (70 eV) m/z: (M+), 314.10 (100%).

**5-(4-chloro-phenyl)-3-(3,4-dimethoxy-phenyl)-4,5-dihydro-pyrazole-1-carbothioic Acid Amide (AP-7):**  $C_{18}H_{18}ClN_3O_2S$  - M.P.: 354 °C; Yield (%): 58; UV ( $\lambda_{max}$ ): 325;  $^1H$  NMR (ppm): 2.0 (s,

2H, S=C-NH<sub>2</sub>), 1.9 (d, 2H, -CH<sub>2</sub>- 4,5-dihydropyrazole), 3.9 (m, 1H, -CH- 4,5-dihydropyrazole), 3.73 (s, 6H, -(O-CH<sub>3</sub>)<sub>2</sub>), 6.7-7.1 (m, 4H, =CH-benzylidininimin), 7.06-7.22 (m, 4H, =CH- benzene); IR (cm<sup>-1</sup>) 3396 (N-H), 2998 (C-H), 1569 & 1458 (C=C Ar), 1508 (C=N), 1265 (C=S), 785 (C-Cl); MS (70 eV) m/z: (M<sup>+</sup>), 375.08 (100%).

**3- (4-bromo-phenyl)- 5-(4-dimethylamino-phenyl)-4, 5-dihydro-pyrazole-1- carbothioic Acid Amide ( AP-8):** C<sub>18</sub>H<sub>19</sub>BrN<sub>4</sub>S - M.P.: 308 °C; Yield (%): 44; UV (λ<sub>max</sub>): 328; <sup>1</sup>H NMR (ppm): 2.0 (s, 2H, S=C-NH<sub>2</sub>), 2.85 (s, 6H, -N-(CH<sub>3</sub>)<sub>2</sub>), 1.9 (d, 2H, -CH<sub>2</sub>- 4,5-dihydropyrazole), 3.9 (m, 1H, -CH- 4,5-dihydropyrazole), 3.73 (s, 6H, -(O-CH<sub>3</sub>)<sub>2</sub>), 7.5 (m, 4H, =CH- benzylidininimin), 6.54-6.94 (m, 4H, =CH- benzene); IR (cm<sup>-1</sup>) 3413 (N-H), 2935 (C-H), 1559 & 1413 (C=C Ar), 1521 (C=N), 1363 (C=S), less than 667 (C-Br); MS (70 eV) m/z: (M<sup>+</sup>), 404.05 (100%).

**3-(2-bromo -4-methoxy-phenyl)-5-(3, 4-dimethoxy -phenyl)-4, 5-dihydro-pyrazole-1 carbothioic Acid Amide (AP-9):** C<sub>19</sub>H<sub>20</sub>BrN<sub>3</sub>O<sub>3</sub>S - M.P.: 328-330 °C; Yield (%): 38; UV (λ<sub>max</sub>): 310; <sup>1</sup>H NMR (ppm): 2.0 (s, 2H, S=C-NH<sub>2</sub>), 1.9 (d, 2H, -CH<sub>2</sub>- 4,5-dihydropyrazole), 3.9 (m, 1H, -CH- 4,5-dihydropyrazole), 3.73 (s, 9H, -O-CH<sub>3</sub> (benzylidininimin), O-(CH<sub>3</sub>)<sub>2</sub>(benzene), 6.7-7.4 (m, 4H, =CH- benzylidininimin), 6.52-6.61 (m, 4H, =CH- benzene); IR (cm<sup>-1</sup>) 3369 (N-H), 2964 (C-H), 1647 & 1458 (C=C Ar), 1558 (C=N), 1265 (C=S), less than 667 (C-Br); MS (70 eV) m/z: (M<sup>+</sup>), 451.04 (100%).

**3-(4-bromo-phenyl)- 5-(4-chloro-phenyl)-4, 5-dihydro-pyrazole-1-carbothioic Acid Amide (P-10):** C<sub>16</sub>H<sub>13</sub>BrCl N<sub>3</sub>S - M.P.: 334-336 °C; Yield (%): 40; UV (λ<sub>max</sub>): 330; <sup>1</sup>H NMR (ppm): 2.0 (s, 2H, S=C-NH<sub>2</sub>), 1.9 (d, 2H, -CH<sub>2</sub>- 4,5-dihydropyrazole), 3.9 (m, 1H, -CH- 4,5-dihydro-pyrazole), 7.5 (m, 4H, =CH- benzylidininimin), 7.01-7.22 (m, 4H, =CH- benzene); IR (cm<sup>-1</sup>) 3446 (N-H), 2969 & 2921 (C-H), 1570 & 1455 (C=C Ar), 1364 (C-N), 1216 (C=S), 785 (C-Cl), less than 667 (C-Br); MS (70 eV) m/z: (M<sup>+</sup>), 394.97 (100%).

## MATERIALS AND METHODS:

***In-vitro* EGFR Inhibitory Assay:** The *in-vitro* anticancer activity of compounds was determined by using EGFR kinases solid-phase ELISA assay.

A 1.6 kb cDNA encoded for the EGFR cytoplasmic domain (EGFR-CD, amino acids 645–1186) was cloned into the baculoviral expression vector pFASTBacHTc. A sequence that encodes (His) 6 was located at the 50 upstream to the EGFR sequence. Sf-9 cells were infected for 3 days for protein expression. Sf-9 cell pellets were solubilized at 00C in a buffer at pH 7.4 containing 50 mM HEPES, 10 mM NaCl, 1% Triton, 10 μM Ammonium Molybdate, 100 μM Sodium Vanadate, 10 μg/mL aprotinin, 10 μg/mL leupeptin, 10 μg/mL pepstatin, and 16 μg/mL benzamidine HCl for 20 min followed by 20 min centrifugation.

Crude extract supernatant was passed through a super equilibrated flow packed column and washed with 10 mM and then 100 mM imidazole to remove nonspecifically bound material. Histidine tagged proteins were eluted with 250 and 500 mM imidazole and dialyzed against 50 mM NaCl, 20 mM HEPES, 10% glycerol, and 1 μg/mL each of aprotinin, leupeptin, and pepstatin for 2 h. The entire purification procedure was performed at 4 °C or on ice. The EGFR kinase assay was set up to assess the level of autophosphorylation based on Time-Resolved Fluorometry.

Compounds AP-1 to AP-10 were dissolved in 100% DMSO and diluted to the appropriate concentrations with 25 mM HEPES at pH 7.4. In each well, 10 μL of the compound was incubated with 10 μL (12.5 ng for HER-2 or 5 ng for EGFR) of the recombinant enzyme (1:80 dilution in 100 mM HEPES) for 10 min at room temperature. Then, 10 μL of 5 mM buffer (containing 20 mM HEPES, 2 mM MnCl<sub>2</sub>, 100 μM Na<sub>3</sub>VO<sub>4</sub> 1 mM DDT and 20 μL of 0.1 mM ATP-50 mM MgCl<sub>2</sub> was added for 1 h. Positive and negative controls were included in each plate by incubation of the enzyme with or without ATP-MgCl<sub>2</sub>. At the end of incubation, the liquid was aspirated, and plates were washed three times with wash buffer. A 75 μL (400 ng) sample of europium labeled anti-phosphotyrosine antibody was added to each well for another 1 h of incubation. After washing, the enhancement solution was added, and the signal was detected by Victor (Wallac Inc.) with excitation at 340 nm and emission at 615 nm. The percentage of autophosphorylation inhibition by the compounds was calculated using the following equation:

100% - [(negative control) / (positive control – negative control)]

The IC<sub>50</sub> was obtained from curves of percentage inhibition with eight concentrations of compounds. As the contaminants in the enzyme preparation are fairly low, the majority of the signal detected by the anti-phosphotyrosine antibody is from EGFR.

**CONCLUSION:** It was observed from the selected QSAR models that biological activities of derivatives are governed by thermodynamic, electronic, and steric properties of the molecules. The models also suggest the groups responsible for increasing the activity. This information can be explored for the designing of new molecules having better anticancer activity.

**ACKNOWLEDGEMENT:** Authors are thankful to Computational and Synthetic Chemistry Division, Department of Pharmaceutical Chemistry, VNS Faculty of Pharmacy, Bhopal for providing the necessary facilities & guidance to carry out this research.

**CONFLICTS OF INTEREST:** Authors have no conflicts of interest while preparing the manuscripts.

#### REFERENCES:

1. Chelysheva E, Turkina A, Evgenia P, Shmakov R, Zeifman A and Sergey A: Placental transfer of tyrosine kinase inhibitors used for chronic myeloid leukemia treatment. *Leukemia & Lymphoma*. 2018; 59: 733-38.
2. Molnar M, Brambhatt H, Rastija V and Komar M: Environmentally Friendly approach to Knoevenagel condensation of rhodamine in choline chloride: urea deep eutectic solvent and QSAR studies on their antioxidant activity. *Molecules* 2018; 23: 1892-97.
3. Halise IG, Cem Y, Gulsen G, Hiroshi S and Hajime K: Cytotoxicity, apoptosis and QSAR studies of phenothiazine derived methoxylated chalcones as anticancer drug candidates. *Medi Chem Res* 2018; 27: 2366-78.
4. Abd El-Gali EA, Mohamed HAG, Gaber OM, Mohamed AAO and Nossier ES: Design, Synthesis and docking studies of novel macrocyclic pentapeptides as anticancer multi-targeted kinase inhibitors. *Mole* 2018; 23: 2410-16.
5. Bandgar BP, Gawande SS, Bodade RG, Totre JV and Khobragade CN: Synthesis and biological evaluation of simple methoxylated chalcones as anticancer, anti-inflammatory and antioxidant agents. *Bioorganic & Medicinal Chemistry* 2010; 18: 1364-70.
6. Sui XC, Bao N, Shaojuan J, John H, John G, Sanjeeva R, Ben T and John D: A role for transferrin receptor in triggering apoptosis when targeted with gambogic acid. *Journal of Medicinal Chemistry* 2013; 46: 2474-81.
7. Maristella CA, Patricia SM, Nelson D and Marcela H: Dehydrocrotonin and its derivative, dimethylamide-crotonin induce apoptosis with lipid peroxidation and activation of caspases-2, -6 and -9 in human leukemic cells HL60. *Toxicology* 2014; 203: 123-37.
8. Lv PC, Wang KR, Li QS, Chen J, Sun J and Zhu HL: Design, synthesis and biological evaluation of chrysin long-chain derivatives as potential anticancer agents. *Bioorganic & Medicinal Chemistry* 2015; 18: 1117-23.
9. Polyakova M, Mei Jin V and Ho Row K: QSPR Models for Chromatographic Retention of some Azoles with Physicochemical properties. *Bulletin of the Korean Chemical Society* 2014; 27: 211-18.
10. Xu JL, Gao SL, Zhang XF, Xie YP, Huang XY and Xie XG: QSAR Studies on 7-Substituted Fluoro-quinolones. *Chinese J of Stru Chemistry* 2015; 26: 91-97.
11. Vasanthanathan P, Lakshmi M, Babu M, Gupta A and Kaskhedikar S: QSAR Study of 3-Phenyl-5-acyloxy methyl-2H, 5H-furan-2-ones as Antifungal Agents. *Chemical and Pharmaceutical Bulletin* 2013; 54: 583-87.

#### How to cite this article:

Singh A and Singour PK: QSAR studies, synthesis and biological evaluation of pyrazole derivatives containing thiourea as tyrosine kinase inhibitors: an approach to design anticancer agents. *Int J Pharm Sci & Res* 2020; 11(9): 4388-94. doi: 10.13040/IJPSR.0975-8232.11(9).4388-94.

All © 2013 are reserved by the International Journal of Pharmaceutical Sciences and Research. This Journal licensed under a Creative Commons Attribution-NonCommercial-ShareAlike 3.0 Unported License.

This article can be downloaded to **Android OS** based mobile. Scan QR Code using Code/Bar Scanner from your mobile. (Scanners are available on Google Play store)